HHS Public Access

Author manuscript

J Immunol. Author manuscript; available in PMC 2016 August 15.

Published in final edited form as:

J Immunol. 2015 August 15; 195(4): 1628–1636. doi:10.4049/jimmunol.1500778.

Natural anti-infective pulmonary proteins: In vivo cooperative action of surfactant protein SP-A and the lung antimicrobial peptide SP-B^{N} (1)

Juan Manuel Coya[*,†], **Henry T. Akinbi**[‡], **Alejandra Sáenz**[*,†], **Li Yang**[‡], **Timothy E. Weaver**[‡], and **Cristina Casals**[*,†,ξ]

[*]Department of Biochemistry and Molecular Biology I, Complutense University of Madrid, 28040-Madrid, Spain

[†]Centro de Investigación Biomédica en Red de Enfermedades Respiratorias (CIBERES), Instituto de Salud Carlos III, 28029-Madrid, Spain

[‡]Division of Pulmonary Biology, Cincinnati Children's Hospital Medical Center and University of Cincinnati College of Medicine, Cincinnati, OH 45229, USA

Abstract

The anionic antimicrobial peptide SP-B^{N}, derived from the N-terminal saposin-like domain of the SP-B proprotein, and SP-A are lung anti-infective proteins. SP-A-deficient mice are more susceptible than WT mice to lung infections, and bacterial killing is enhanced in transgenic mice overexpressing SP-B^{N}. Despite their potential anti-infective action, *in vitro* studies indicate that several microorganisms are resistant to SP-A and SP-B^{N}. In this study we test the hypothesis that these proteins act synergistically or cooperatively to strengthen each other's microbicidal activity. The results indicate that the proteins acted synergistically *in vitro* against SP-A- and SP-B^{N}-resistant capsulated *Klebsiella pneumoniae* (serotype K2) at neutral pH. SP-A and SP-B^{N} were able to interact in solution (K_d = 0.4 μM), which enabled their binding to bacteria with which SP-A or SP-B^{N} alone could not interact. *In vivo*, we found that treatment of *K. pneumoniae*-infected mice with SP-A and SP-B^{N} conferred more protection against *K. pneumoniae* infection than each protein individually. SP-A/SP-B^{N}-treated infected mice showed significant reduction of bacterial burden, enhanced neutrophil recruitment, and ameliorated lung histopathology with respect to untreated infected mice. In addition, the concentrations of inflammatory mediators in lung homogenates increased early in infection in contrast with the weak inflammatory response of untreated *K. pneumoniae*-infected mice. Finally, we found that therapeutic treatment with SP-A and SP-B^{N} 6h or 24h after bacterial challenge conferred significant protection against *K. pneumoniae* infection. These studies show novel anti-infective pathways that could drive development of new strategies against pulmonary infections.

(1)This work was supported by Spanish Ministry of Economy and Competitiveness (SAF2012-32728) and Institute of Health Carlos III, (ISCiii) (Spanish Research Center of Respiratory Diseases, CIBERES CB06/06/0002). This work was also supported by an award from The National Institutes of Health, HL103923 (TEW)

ξTo whom correspondence should be addressed: Cristina Casals, Department of Biochemistry and Molecular Biology I, Faculty of Biology, Complutense University of Madrid, 28040 Madrid, Spain, Tel.: (34) 913944261, Fax: (34) 913944672, ccasalsc@ucm.es.

INTRODUCTION

Klebsiella pneumoniae is a well-known opportunistic pathogen that may be responsible for as much as 8% of all hospital-acquired infections (1). The emergence of multidrug-resistant strains of *K. pneumoniae* has significantly complicated the management and treatment of infections involving this organism by contributing to increased bacterial drug resistance, toxic effects, and health care costs (1). The pipeline for new antibiotics is insufficient to match the health burden posed by lung infection and the effectiveness of current therapeutic strategies against pneumonia is threatened (2).

Endogenous antimicrobial peptides possess desirable features of new classes of antibiotics, including broad spectrum activity, neutralization of endotoxins, activity *in vivo*, and possible synergy with one another and with antibiotics (3). Consequently, a variety of host defense proteins are gaining considerable attention and clinical interest because of their importance in maintaining lung homeostasis in ambient conditions and their potential to kill multidrug-resistant microorganisms. Among these proteins, SP-A and the NH_2-terminal segment of the surfactant protein B propeptide (SP-B^N) have been shown to be potent innate immune molecules in the lung (4, 5).

SP-A is a large protein, secreted into the alveolar fluid, which plays a key role in lung innate immunity. It enhances phagocytosis of microorganisms by opsonization or direct alveolar macrophage stimulation (4). It is able to regulate inflammatory mediator production depending upon the pathogen, the responding host cell, and the cytokine environment (4). In addition, it has been demonstrated that SP-A has a potent macrophage-independent antibacterial activity *in vivo* (6) and SP-A deficiency in gene-targeted mice causes increased susceptibility to lung infections (4). This antimicrobial property is shared with antimicrobial peptides present in the alveolar space such as SP-B^N, an ~80-amino acid saposin-like peptide, which is secreted into the air space together with surfactant components (5). *In vitro*, SP-B^N indirectly promotes the phagocytosis of bacteria by macrophage cell lines, and it directly kills bacteria at acidic, but not at neutral pH, consistent with a lysosomal antimicrobial function (5). Moreover, overexpression of SP-B^N in the distal airway epithelium protects mice against infection with *Pseudomonas aeruginosa* and *Streptococcus pneumonia* (5).

Despite the potential anti-infective action of SP-A and SP-B^N in the lung, a number of questions remain unanswered, including the mechanism by which SP-B^N might kill bacteria in the alveolar fluid at neutral pH, or the factors that govern SP-A's anti-microbial activity since *in vitro* studies indicate that several microorganisms are resistant to SP-A (7). It is possible that cooperative interactions of SP-A with other antimicrobial peptides or proteins present in the alveolar fluid enhance the microbicidal defense of the lungs; yet little is known about *in vivo* interactions between soluble factors and SP-A and their relevance in innate host defense.

In this study we investigate the potential interaction of SP-A and SP-B^N in airway host defense. Results show the concerted antimicrobial action of SP-A and SP-B^N *in vitro* and *in vivo* against *Klebsiella pneumoniae* K2 infection and the therapeutic benefit of SP-A/SP-B^N

treatment after bacterial challenge, suggesting that harnessing the host's natural antimicrobial proteins might provide an adjunct to the current therapy for pneumonia.

METHODS

SP-B^N and SP-A

Recombinant human SP-B^N (MW, 8 KDa) was expressed in *Escherichia coli* BL21 (DE3) and purified over a Ni-NTA agarose column (Novagen) as previously described (5). Human surfactant protein A was isolated from bronchoalveolar lavage (BAL) of patients with alveolar proteinosis using a sequential butanol and octylglucoside extraction (8-10). The purity of SP-A and SP-B^N was verified by 1-dimensional SDS-PAGE in 12% acrylamide under reducing conditions. In addition, human SP-A was characterized by intrinsic fluorescence spectroscopy (8) and dynamic light scattering (DLS) (9). The oligomerization state of SP-A was assessed by electrophoresis under nondenaturing conditions (8, 10), electron microscopy (8), and analytical ultracentrifugation as reported elsewhere (10). SP-A consisted of supratrimeric oligomers of at least 18 subunits (MW, 650 KDa). Biotinylated SP-A and SP-B^N were prepared as previously described (9). The structure and functional activity of biotinylated proteins were similar to those of unlabeled SP-A and SP-B^N. The endotoxin level of each protein was measured by the limulus amebocyte lysate endotoxin assay kit according to the manufacturer's instructions (GenScript, USA). Endotoxin levels of the proteins were less than 0.15 EU/ml.

Mice, Bacteria, and Cell Lines

Five- to six-week old male FVB/N were purchased from The Jackson Laboratory, Bar Harbor, ME. All mice were housed in a pathogen-free barrier facility and were handled according to the Institutional Animal Care and Use Committee guidelines at Cincinnati Children's Hospital Medical Center.

Klebsiella pneumoniae strain K2 (from Dr. Korfhagen, Cincinnati Children's Hospital) and the clinical isolate *Klebsiella pneumoniae* 52145 strain K2 (from Dr. Bengoechea, Queen's University Belfast) were used in the current study. Both bacteria are heavily encapsulated and particularly virulent in mice. In addition, we used a K. pneumoniae 52145 isogenic mutant nonexpressing capsule (11) provided by Dr. Bengoechea. To minimize variability in virulence, all bacteria were selected from aliquots of the same passage stored at −70 °C in 16% glycerol/trypticase soy broth (TSB). All bacteria were grown in Luria-Bertani (LB) at 37 °C.

Mouse alveolar (MH-S) and peritoneal (Raw 264.7) macrophages were purchased from American Type Culture Collection (Rockville, MD). Both were grown at 37 °C and 5% CO_2 in RPMI 1640 medium supplemented with 2mM glutamine, 100 units/ml penicillin, 100 units/ml streptomycin, and 10% fetal bovine serum (FBS).

Phagocytosis and bacterial killing assay *in vitro*

Bacteria were grown in LB at 37 °C with continuous shaking to exponential phase. Bacteria were then harvested, re-suspended in PBS, and adjusted to the desired final concentration.

For phagocytosis assays, MH-S or RAW 264.7 cells were seeded in 24-well tissue culture plates at a density of 3×10^5 cells per well 15 h before each experiment. Macrophages were subsequently pre-incubated 4 h with or without different concentrations of SP-A (25, 50, and 100 μg/ml), SP-B^N (5, 10, and 20 μg/ml), or combinations of both, and then washed twice with PBS before 1h infection with *K. pneumoniae* K2 (5×10^7 CFU). In another set of experiments, bacteria (5×10^7 CFUs) were pre-incubated in the presence or absence of SP-A (100 μg/ml) and/or SP-BN (20 μg/ml) for 2h before being added to Raw 264.7 or MH-S macrophages. Then, cells were infected with *K. pneumoniae* K2. After 1h of infection, monolayer cells were washed 3 times with PBS and incubated with RPMI containing 10% FCS, 10 mM Hepes, gentamicin (300 μg/ml), and polymyxin B (15 mg/ml) for 90 minutes to kill extracellular bacteria. Cells were washed to remove gentamicin and polymyxin, lysed with 0.5% saponin, and re-suspended in PBS. The lysates were diluted serially for CFU enumeration of viable bacteria.

To evaluate the microbicidal activity of SP-A and SP-B^N, colony counts on plate assays were used. Five microliters of bacterial suspension were incubated with different concentrations of SP-A (25, 50, and 100 μg/ml), SP-B^N (2.5, 5, 10, and 20 μg/ml), or combinations of both in 20 mM phosphate, 150 mM NaCl buffer, pH 7.0, or 5 mM sodium acetate buffer, pH 5.5 during 1 h at 37 °C. These experiments were also carried out with the same buffers with or without 2 mM Ca^{2+}. In all cases the final bacterial concentration was 10^5 CFU/ml. At the end of incubation, bacterial suspensions were plated on LB agar plates and incubated for 18 h at 37 °C. Viable bacteria were enumerated by colony count.

Binding assays

SP-A and SP-B^N binding to bacteria—To explore the ability of biotinylated SP-A or biotinylated SP-B^N to bind *K. pneumoniae* K2 in the presence of SP-B^N or SP-A, respectively, binding assays were performed as previously described (12) with slight modifications. Briefly, 10^7 CFU/ml of *K. pneumoniae* K2 in 5 mM Tris buffer, pH 7.4, containing 150 mM NaCl and 2 mM Ca^{2+} were incubated with several concentrations of biotinylated SP-A (0 to 1.3 μg/ml) or biotinylated SP-B^N (0 to 5 μg/ml) in the presence or absence of the indicated protein (SP-B^N, SP-A, or human serum albumin (HSA)) by gentle orbital rotation for 30 min at room temperature. In some experiments, the buffer was replaced by 5 mM sodium acetate buffer, pH 5.5, in the binding and washing steps. In all cases, bacteria were pelleted, washed twice, and resuspended in 200 μl of carbonate buffer 0.1 M, pH 9.5. Controls were performed in absence of bacteria to estimate nonspecific binding. Protein binding was analyzed by solid-phase binding as follows. Samples were applied to a 96 well-plate maxisorp (Nunc, Rochester, NY, USA) and allowed to bind 1 h at 37 °C. The plate was blocked with 5mM Tris HCl containing 10 % FBS for 1 h at 37°C. After extensive washing, streptavidin-horseradish peroxidase was added to the wells and incubations were performed for 1 h at room temperature. Biotinylated protein detection was performed by adding *3,3′,5,5′-tetramethylbenzidine liquid substrate* (TMB; Sigma). The colorimetric reaction was halted with 4 M sulfuric acid, and the absorbance was read at 450 nm on an ELISA reader (DigiScan; Asys HiTech GmbH, Eugendorf, Austria). The results obtained were expressed as nanograms of bound-protein/10^7 bacteria.

SP-B^N binding to SP-A—To explore whether SP-B^N binds to immobilized SP-A, solid-phase binding assay was performed with biotinylated SP-B^N. Wells of a 96-well maxisorp microtiter plate (Nunc, Rochester, NY, USA) were coated with either SP-A (25 μg) or HSA (25 μg) in 0.1 mM sodium bicarbonate buffer, pH 9.5, overnight at 4°C. Wells were washed (5 mM Tris HCl, pH 7.4, containing 150 mM NaCl, 2 mM $CaCl_2$, and 0.1% Tween 20) and blocked with washing buffer containing 2.5% non-fat dried milk for 2 h. Subsequently, biotinylated SP-B^N in concentrations ranging from 0 to 6 μM was added to the wells and incubated in the same buffer for 1 h at room temperature. To detect SP-A-bound biotinylated SP-B^N, streptavidin-horseradish peroxidase was added as described above.

Intrinsic fluorescence experiments—Tryptophan SP-A fluorescence measurements to explore the binding between SP-A and SP-B^N in solution were carried out as previously described (13), using an SLM-Aminco AB-2 spectrofluorimeter equipped with a thermostat-regulated cuvette holder (±0.1 °C; Thermo Spectronic, Waltham, MA, USA) in quartz cuvettes with 5 × 5 mm path length. The slit widths were 4 nm for the excitation and emission beams. The tryptophan fluorescence emission spectrum of SP-A (15 nM) was recorded from 305 to 400 nm on excitation at 295 nm at 25 °C in 5 mM Tris HCl buffer (pH 7.4) containing 150 mM NaCl. Subsequently, the titration experiment was started by adding increasing amounts of SP-B^N to the protein solution in the cuvette. The fluorescence intensity readings were corrected for the dilution caused by SP-B^N addition.

The data from equilibrium binding titrations of SP-A were analyzed by nonlinear least-squares fitting to equation (1):

$$\Delta F = \Delta F_{max} \cdot \frac{[\text{peptide}]^n}{K_d + [\text{peptide}]^n} \quad (1)$$

where ΔF is the change in fluorescence emission intensity at 335 nm relative to the intensity of free SP-A; ΔF_{max} is the change in fluorescence intensity at saturating SP-B^N concentrations; K_d is the apparent equilibrium dissociation constant; [peptide] is the molar concentration of free SP-B^N; and n is the Hill coefficient.

Dynamic light scattering (DLS)—The hydrodynamic diameters of SP-B^N and SP-A particles as well as mixtures of these components were measured at 25 °C in a Zetasizer Nano S from Malvern Instruments (Worcestershire, UK) equipped with a 633 nm HeNe laser, as previously described (9). The interaction of SP-A with SP-B^N in solution was measured by addition of different concentrations of SP-B^N (from 0 to 5.5 μM) to a fixed concentration of SP-A (10 nM), in 20 mM phosphate buffer, pH 7.4, with or without 150 mM NaCl. Experiments were also performed in 5 mM sodium acetate buffer, pH 5.5.

Bacterial killing *in vivo*

Preliminary experiments identified a dose of intratracheal *K. pneumoniae* K2 that caused lung inflammation with minimal mortality in WT FVB/N mice. Ten thousand CFUs of *K. pneumoniae* K2 were administered intratracheally as previously described (13).To assess the concerted action of SP-A and SP-B^N *in vivo*, a combination of *K. pneumoniae* K2 and either SP-A, SP-B^N, or both proteins resuspended in 100 μL of 5 mM Tris HCl, 150 mM NaCl, pH

7.4, were administered intratracheally to mice. Mice were sacrificed at 6h or 24h post-infection. For therapeutic application of SP-A/SP-B^N, mice infected with *K. pneumoniae* were treated with SP-A+SP-B^N 6h or 24h after the bacterial challenge. Mice were sacrificed at 24 h or 48 h post-infection, respectively. In both applications, after infection time, lungs were harvested, weighed, and homogenized in 1 ml sterile PBS. For *in vivo* studies, an appropriate concentration of SP-A (150 nM) and SP-B^N (2.5 μM) was used. Dilutions of lung homogenates were plated on LB agar plates and the number of CFUs determined after an overnight incubation at 37°C. Each experimental group included 6 mice and data were expressed as CFU ± SEM/mouse.

Lung histopathology

Mice were exsanguinated and their lungs were inflation-perfused with paraformaldehyde, excised and further fixed with 4% paraformaldehyde for 24 h. Fixed tissues were embedded in paraffin, and 5 μm sections were prepared and stained with hematoxylin and eosin, as previously described (14, 15)

Bronchoalveolar lavage cell count

WT FVB/N infected mice (untreated or treated with SP-A and/or SP-B^N) were exsanguinated and their lungs were then lavaged three times with 1-ml aliquots of sterile PBS. BAL fluid was centrifuged at 2000 × g for 10 min, and the pellet was resuspended in 0.5 ml of PBS as described previously (14). A 50-μl aliquot was stained with an equal volume of 0.4% trypan blue (Life Technologies) for total cell count on a hemocytometer. Differential cell counts were made on cytospin preparations stained with Diff-Quik (Scientific Products, McGraw Park, IL).

Cytokine levels in lung homogenates

At 6 or 24 hours after bacterial inoculation, levels of cytokines associated with severe lung injury (mouse IL-1β, IL-6, IL-17α, TNF-α, and MIP-2) were assessed in lung homogenates by enzyme-linked immunosorbent assay (ELISA) using MilliplexTM Multiplex kits (Millipore, Billerica, MA) according to manufacturer's protocol.

Statistical analysis

Data are presented as means ± SD (in vitro experiments) or SEM (in vivo experiments). Differences in means between groups were evaluated by one-way ANOVA followed by the Bonferroni multiple-comparison test. For comparison of two groups, Student t test was used. An α level ≤ 5% ($p \leq 0.05$) was considered significant.

RESULTS

Synergic actions of SP-B^N and SP-A against *Klebsiella pneumoniae* K2 at neutral pH

To assess potential synergistic interaction between SP-B^N and SP-A in *K. pneumoniae* killing, capsulated K2 (WT) and non-capsulated bacteria were incubated with increasing concentrations of SP-B^N in the absence or presence of SP-A (100 μg/ml) at pH 7.4, and colony count assays were performed. Fig. 1A shows that neither SP-B^N nor SP-A alone was

able to kill capsulated or non-capsulated *K. pneumoniae* at neutral pH; however, in combination, SP-A and SP-B^N effectively killed capsulated and non-capsulated *K. pneumoniae* at pH 7.4, indicating that the capsule polysaccharide did not protect bacteria from SP-B^N/SP-A-mediated antimicrobial activity. Addition of 2 mM calcium did not enhance SP-B^N/SP-A-mediated killing (data not shown), indicating that the presence of Ca^{2+} is not essential for bactericidal activity. Given that SP-B^N is able to kill bacteria at acidic pH (5) we also performed killing experiments under these conditions. However, at this pH, the bactericidal action of SP-B^N on *Klebsiella pneumoniae* K2 was not increased by the presence of SP-A (Supplementary Fig. S1.A).

Because SP-A and SP-B^N, individually, have been proven to enhance phagocytosis of several respiratory pathogens (4, 5), we investigated the potential cooperative action between SP-B^N and SP-A to enhance uptake of *K. pneumoniae* K2 by mouse alveolar (MH-S) or peritoneal (Raw 264.7) macrophages. Pre-incubation of these macrophage cell lines with increasing concentrations of SP-B^N (5 to 20 μg/ml) for 4 h prior to the addition of bacteria resulted in a significant increase in viable intracellular bacteria compared with untreated cells. In contrast, preincubation with SP-A (100 μg/ml, 0 μg/ml SP-B^N) had no effect (Fig. 1B). However, pre-incubation of macrophages with SP-A in combination with increasing amounts of SP-B^N resulted in a significant increase in bacterial uptake, compared with untreated cells and cells treated with SP-B^N alone (Fig. 1B). These data suggest that SP-A and SP-B^N act in conjunction to indirectly increase phagocytosis of *K. pneumoniae* by macrophages. On the other hand, we found that bacterial phagocytosis did not increase after 2 h preincubation of *K. pneumoniae* K2 with SP-A+SP-B^N or with each protein separately (data not shown). These experiments indicate that SP-A and/or SP-B^N did not directly trigger *K. pneumoniae* phagocytosis by bacterial opsonization.

To determine the binding of SP-A to *K. pneumonia* K2, bacteria were incubated with biotinylated SP-A (0 to 1.25 μg/ml) in the absence or presence of SP-B^N (10 μg/ml) or HSA (10 μg/ml). SP-A alone was unable to bind *Klebsiella pneumoniae* K2, even in the presence of HSA (Fig. 1C). However, SP-A bound avidly to *K. pneumoniae* in a dose-dependent manner when SP-B^N was added to the solution (Fig. 1C). Similarly, the binding of biotinylated SP-B^N (0 to 5 μg/ml) was determined in the absence or presence of SP-A (100 μg/ml) or HSA (10 μg/ml) (Fig. 1D). Biotinylated SP-B^N alone was able to bind to *K. pneumoniae* K2 at acidic but not neutral pH (Supplementary Fig. S1.B). However, SP-B^N bound avidly to this pathogen in a dose-dependent manner at neutral pH when SP-A was added to the solution (Fig. 1D). Thus, at neutral pH, SP-A and SP-B^N effectively bound to (Figs. 1C & D) and killed (Fig. 1A) *K. pneumoniae* K2 only when presented to the bacteria in combination.

SP-B^N binds directly to SP-A

To understand how SP-A and SP-B^N jointly strengthen each other's microbicidal activity against *K. pneumoniae*, we studied the potential interaction of SP-A and SP-B^N in solution by monitoring changes in the intrinsic fluorescence of SP-A after SP-B^N binding (Fig. 2A). The fluorescence of SP-A is dominated by the contribution of its two conserved tryptophan residues at the COOH-terminal end of the protein. Addition of increasing concentrations of

SP-B^N (0 to 5.5 μM) resulted in a significant SP-B^N concentration-dependent decrease in the amplitude of the fluorescence emission spectrum of SP-A, without any shift in the wavelength of the emission maxima (Fig. 2A). These data suggest that the interaction of SP-B^N with SP-A produces conformational changes in SP-A resulting in a higher level of tryptophan fluorescence quenching by polarizable groups in the proximity of these residues (9, 13). The estimated dissociation constant (K_d) for SP-A/SP-B^N interaction was 0.39 ± 0.02 μM and the Hill coefficient (n) = 1.

The interaction between SP-B^N and SP-A was also examined by solid-phase binding assay. Fig. 2B shows that SP-B^N interacted with immobilized SP-A in a dose-dependent and saturable manner with a K_d of 0.4 ± 0.08 μM. SP-B^N did not bind to wells coated with HSA (Fig. 2B, open circles) or wells containing buffer alone. The K_d obtained by this method was quite similar to that calculated for SP-A and SP-B^N in solution (Fig. 2A).

In addition, we found that the binding of SP-B^N to SP-A at neutral pH caused an SP-B^N concentration-dependent increase of SP-A hydrodynamic size in the presence of salts, as determined by dynamic light scattering (Fig. 2C), resulting in the formation of protein-protein aggregates of 950 ± 50 nm. SP-B^N alone formed large aggregates at acidic but (Supplementary Fig S1.C) not at neutral pH. At acidic pH, SP-A/SP-B^N interaction was not observed (Supplementary Fig S1.C).

Killing of *K. pneumoniae* in mice treated with SP-A and SP-B^N

To determine an appropriate bacterial dose for *in vivo* studies, 10^3 to 10^5 CFUs of *K. pneumoniae* K2 were inoculated intratracheally in wild-type FVB/N mice (6 mice/group). Administration of *Klebsiella* was well tolerated, and all animals survived the 72-h study period at the 10^4 CFUs dose. Alteration in activity or physical appearance of the animals was not detected until 72 h post-infection. *K. pneumoniae* K2 was intratracheally co-administered with SP-A, SP-B^N, or both proteins to WT FVB/N mice and bacterial burden was assessed (Fig. 3). At 6 h post-infection, lung bacterial burden decreased 60% in SP-A- ($p < 0.05$), 56 % in SP-B^N- ($p < 0.05$) and 85 % in SP-A+SP-B^N-treated mice ($p = 0.001$). Bacterial burden was also significantly decreased at 24 h post-infection when mice were treated with SP-A (56 %; $p < 0.05$), SP-B^N (77 %; $p < 0.05$), or SP-A+ SP-B^N (90 %; $p < 0.001$) (Fig. 3), indicating that at the doses used in this study, these proteins are more effective in slowing microbial growth when they are co-administered. At 72 h post-infection, there was no difference among the groups, suggesting that exogenous SP-A and SP-B^N are consumed after 24 h and that retreatment and/or higher doses will be required to control infection.

Lung histopathology and inflammation in SP-A and SP-B^N-treated mice after *K. pneumoniae* infection

There was a modest increase in the total BAL cell counts in mice 24 h, but not 6 h, after infection with *K. pneumonia* K2, compared to uninfected mice treated with vehicle (Fig. 4A). Total cell numbers in BAL from SP-A- or SP-B^N-treated groups were significantly increased at 24 h, but not 6h, post-infection compared to untreated infected animals. Combined SP-A/SP-B^N treatment further enhanced cell recruitment at 24 h post-infection

compared to untreated infected animals ($p < 0.001$) and to infected mice treated with SP-A or SP-B^N alone ($p < 0.001$). Administration of both proteins in uninfected mice did not produce significant changes in BAL cell counts (Fig. 4A).

Histologic examination of lung sections showed mild leukocytic alveolitis in lungs of infected mice at 6h post-infection, which was more pronounced in infected mice treated with SP-A+SP-B^N (Fig. 4B), consistent with neutrophil recruitment (Fig. 5). At 24h post-infection, alveolar and peribronchiolar infiltrates increased in both SP-A/SP-B^N-treated and untreated infected mice. However, areas of lobular pneumonia were more intense in untreated mice (Fig 4B, black arrows). No pathological changes were observed in saline challenged (control) lungs from uninfected mice (Fig. 4B).

Analyses of cell types in BAL from infected mice treated with SP-A+SP-B^N revealed that recruited cells consisted predominantly of neutrophils (Fig. 5). There was no difference in macrophages among the groups regardless of treatment regimen. However, neutrophil recruitment was significantly greater in infected mice treated with SP-A+SP-B^N compared to infected mice treated with SP-A or SP-B^N and untreated infected mice (Fig. 5). Control experiments indicate that neutrophil recruitment did not significantly increase in uninfected mice treated with SP-A+SP-B^N compared to untreated uninfected mice (Fig. 5).

Early neutrophil recruitment was strongly associated with elevated levels of TNF-α, IL-1β, IL-6, MIP-2 ($p<0.001$), and IL-17α ($p<0.05$) (Fig. 6). The cytokine response was detected only in animals treated with SP-A/SP-B^N at 6h post-infection, and was transient, returning to baseline at 24h post-infection. Untreated infected mice showed a weak inflammatory response both at 6 and 24h post-infection (Figs. 5 and 6).

Therapeutic effect of SP-A and SP-B^N in mice with an established infection

To assess the therapeutic potential of SP-A/SP-B^N treatment, WT FVB/N mice were first infected with *K. pneumoniae* K2 and subsequently treated with exogenous proteins 6 or 24h post-infection. Lung bacterial burden and BAL cells were analyzed at either 24 h post-infection (for animals treated 6h after pathogen inoculation) or at 48 h post-infection (for animals treated 24h after inoculation).

Figure 7 shows that SP-A/SP-B^N treatment 6h after bacterial inoculation significantly reduced bacterial burden (67 %; $p < 0.001$) at 24 h post-infection. Moreover, SP-A/SP-B^N treatment after 24 h of pathogen inoculation also decreased bacterial CFUs at 48 h post-infection (72 %; $p < 0.001$). Reduced bacterial burden was associated with increased neutrophil infiltration at 24 h and 48 h post-infection in SP-A/SP-B^N-treated mice compared with untreated infected mice ($p < 0.05$). Therefore, our results indicate that therapeutic treatment with SP-A and SP-B^N conferred a significant protection against *K. pneumoniae* K2 infection.

DISCUSSION

The purpose of this study was to evaluate the potential cooperative action of two components of lung innate host defense: the N-terminal saposin-like domain of the SP-B

proprotein of ~81 amino acid residues, and the large oligomeric protein SP-A. Both are synthesized and proteolytically processed by type II alveolar epithelial cells. Once secreted to the alveolar fluid, the anionic peptide SP-B^N has been detected unassociated with surfactant membranes (5) that are rich in anionic phospholipids, and that sequester cationic, but not anionic, antimicrobial peptides at neutral pH. The anionic peptide SP-B^N shows microbicidal activity only at acidic pH, which is incompatible with its potential extracellular antimicrobial activity. However, elevated SP-B^N concentrations in the airspaces of transgenic mice overexpressing SP-B proprotein were associated with decreased bacterial load and enhanced survival, following intranasal infection with *P. aeruginosa* (5). This suggests that other factors present in the alveolar fluid might act cooperatively with SP-B^N, reinforcing the microbicidal defense of the lungs.

We hypothesize that SP-B^N binding to SP-A, a versatile recognition protein that binds to a great variety of immune and non-immune ligands (4), synergizes antimicrobial activity. Our results indicate that both proteins were able to interact at neutral pH in the presence of salts (K_d = 0.4 μM). This protein-protein interaction allowed SP-A/SP-B^N to bind to pathogenic *K. pneumoniae* K2 in vitro at pH 7.4 (while neither of these proteins bound to *K. pneumoniae* K2 alone) and kill bacteria at neutral pH. Moreover, SP-A/SP-B^N complexes indirectly increased phagocytosis of *K. pneumoniae* by macrophages. In addition, cooperative interaction between SP-A and SP-B^N against *K. pneumoniae* K2 was demonstrated *in vivo*. Importantly, the antimicrobial action of SP-A and SP-B^N, administered 6 or 24h after pathogen inoculation, suggests that exogenous administration of recombinant SP-A and SP-B^N may be of therapeutic benefit.

Several reports have suggested the importance of cooperative interaction between mammalian antimicrobial defenses (16). However, little is known about the biological basis of interactions among several soluble factors and between soluble factors and pathogens in the airways and alveolar space. Soluble factors that do not interact with each other might act additively against pathogens, whereas molecular interactions between soluble factors might facilitate or impede their biological activities. In the alveolar fluid, lactoferrin and lysozyme have been proven to act synergistically, while hβD-2 and human cathelicidin act additively against E. coli (17). Synergistic activity in triple combinations of lysozyme, lactoferrin, and the protease inhibitor secreted by leukocytes has also been reported (17). Moreover, SP-A and SP-D have been shown to have additive neutralizing activity with cathelicidin against influenza A virus (18). Our results suggest that synergistic interaction of SP-A and SP-B^N might be important to overcome Gram-negative bacterial infections in the alveolar airspaces.

With respect to structural characteristics of SP-B^N, this peptide has a B-type saposin module. Saposin B contains three strictly conserved intramolecular disulfide bridges that stabilize a saposin-fold, composed of amphipathic helices. The three-dimensional structure of saposin B reveals an unusual shell-like dimer consisting of a monolayer of α-helices enclosing a large hydrophobic cavity (19). Most of the hydrophobic residues that line the concave surface of the monomers remain exposed to a large interior cavity, and the protein does not have a packed hydrophobic core. The existence of the large hydrophobic cavity suggests extraction of target lipids from membranes with which saposins interact (19). SP-B^N as well as saposin B is negatively charged. Thus its interaction with negatively charged

bacterial capsules and membranes (such as LPS) is pH dependent. Low pH would trigger the protonation and neutralization of negatively-charged residues of SP-B^N, which would otherwise avoid binding to anionic bacterial capsules or bacterial membranes. In addition, SP-B^N underwent pH-dependent aggregation that might be relevant for its antimicrobial activity at acidic pH (5).

On the other hand, SP-A is a large extracellular protein structurally characterized by an N-terminal collagen-like domain connected by a neck segment with globular C-terminal domains that include a C-type carbohydrate recognition site (4). SP-A is assembled in multiples of three subunits due to its collagen domain and its supratrimeric assembly has a bouquet-type structure similar to mannose binding protein or C1q (4, 8). We previously found that SP-A permeabilizes model bacterial membranes by forming calcium-dependent protein aggregates that may extract lipids from the membrane at neutral pH. As a consequence, transient defects are produced, rendering the bacterial membrane leaky (20). In this study we found that the binding of SP-B^N to SP-A at neutral pH caused SP-A-conformational changes and an increase of the protein hydrodynamic size that is dependent on SP-B^N concentration. SP-B^N binding to SP-A resulted in the formation of protein aggregates of 950 ± 50 nm. SP-A/SP-B^N complexes effectively killed *K. pneumoniae* K2 *in vitro* at neutral pH, in contrast to SP-A or SP-B^N alone. The mechanism by which SP-A and SP-B^N produce bacterial death synergistically remains to be determined. It is possible that NaCl-dependent binding of SP-B^N to SP-A would trigger the neutralization of negatively charged residues of SP-B^N, which would otherwise hinder SP-B^N binding to the anionic bacterial capsule and/or LPS. In addition, SP-A/SP-B^N complexes could form a type of fiber that might destabilize the bacterial capsule and/or the outer bacterial membrane. Importantly, SP-B^N alone also formed aggregates at acidic pH as determined by DLS, and SP-B^N oligomers were able to kill *K. pneumoniae* K2. Significantly, a number of antimicrobial peptides (such as protegrin-1, dermaseptin S9, and temporins B and L) have been reported to form fibrillar aggregates (21, 22), suggesting a possible mechanistic connection between protein/peptide aggregation and antimicrobial activity.

Combined SP-A/SP-B^N intratracheal administration to mice infected with *K. pneumoniae* K2 conferred more protection against bacterial infection than each protein individually, measured at 6h and 24h post-infection. SP-A/SP-B^N-treated infected mice showed significant reduction of bacterial burden in comparison to untreated infected mice. Exogenous SP-A or SP-B^N, administered alone, also showed protection against infection even though *K. pneumoniae* K2 is resistant to either SP-A or SP-B^N *in vitro* at neutral pH. This is likely due to the presence in the alveolar fluid of endogenous proteins/peptides that strengthen their antimicrobial actions.

The ability of SP-A and SP-B^N to enhance clearance of *K. pneumoniae* K2 *in vivo* could be related to their capability to both kill bacteria and modulate host inflammatory response. Thus the antibacterial activity of SP-A/SP-B^N in *K. pneumoniae* K2-infected mice was accompanied by increased early neutrophil recruitment in BAL, which is consistent with the enhancement of an early inflammatory response. Untreated infected mice showed a weak neutrophil influx into the lung at both 6 and 24h post-infection and a lack of an early inflammatory response in mice lungs. This finding is consistent with the fact that *K.*

pneumoniae K2 antagonizes the activation of NF-kB in order to subvert the host inflammatory response for its own benefit (23, 24). Several reports have demonstrated that activation of host inflammatory response is essential to clear *Klebsiella pneumoniae* infection (25, 26), and we found that SP-A and SP-B^N were able to enhance early inflammatory response to *K. pneumoniae* K2. SP-A/SP-B^N boosted the expression of several pro-inflammatory cytokines (TNF-α, IL-1β, IL-6, IL-17-α, and MIP-2) at 6h post inflection. This is consistent with SP-A/SP-B^N-induced recruitment of neutrophils to the alveolus, which can eliminate resistant pathogens by intra- and extracellular mechanisms (27).

Results also indicate that exogenous SP-B^N, but not SP-A, treatment was effective in neutrophil recruitment. Although data supporting the role of SP-B^N in inflammation are sparse, anionic antimicrobial peptides have been shown to induce cytokine and chemokine production. Dermcidin is an antimicrobial peptide secreted into sweat, which shares some features with SP-B^N such as anionicity, antimicrobial activity at acidic pH, and constitutive expression. Dermcidin-derived peptides have been shown to activate normal human keratinocytes by inducing pro-inflammatory and chemoattractive mediators (28). In addition, cationic antimicrobial peptides have been reported to promote chemotaxis, both indirectly by stimulating the expression of chemokines and directly by acting as chemokines themselves to recruit a variety of immune cells (29).

Interestingly, the early proinflammatory response induced by SP-A/SP-B^N treatment to infected mice was transient, returning to baseline at 24h post-infection. It is remarkable that the number of alveolar macrophages did not change in infected groups, regardless of treatment regimen, compared to uninfected mice. Alveolar macrophages ingest apoptotic neutrophils recruited in the alveolar space after pathogen challenge, and SP-A enhances the clearance of apoptotic neutrophils (30), promoting the resolution of inflammation. It is believed that SP-A plays a significant role in tipping the balance of inflammation to protect the alveolar epithelium while facilitating pathogen clearance, although the molecular mechanisms by which SP-A interacts with various immune cells are poorly understood.

In summary, we found that lung surfactant-derived components SP-A and SP-B^N act in conjunction to protect the lungs against *K. pneumoniae* K2 infection. Our data indicate that SP-A and SP-B^N in combination directly kill *K. pneumoniae* K2. SP-A/SP-B^N treatment significantly reduces bacterial burden and enhances endogenous protective mechanisms to aid in the clearance of bacteria. In addition, SP-A/SP-B^N treatment after 24h of pathogen inoculation significantly decreases bacterial burden at 48h post-infection. Therefore, our data indicate that therapeutic treatment with SP-A and SP-B^N confers significant protection against *K. pneumoniae* K2 infection. Given the alarming increase in multidrug-resistant Gram-negative bacteria in the face of a paucity of new antibiotics, we have shown that naturally occurring lung proteins may provide a novel model of adjunctive therapy for Gram-negative bacterial infections.

Supplementary Material

Refer to Web version on PubMed Central for supplementary material.

ACKNOWLEGMENT

We thank Alyssa Sproles of Research Flow Cytometry at Cincinnati Children's Hospital Medical Center for her assistance. We also thank Dr. Korfhagen (Cincinnati Children's Hospital) for providing *Klebsiella pneumoniae* strain K2 and Dr. Bengoechea (Queen's University Belfast) for providing *Klebsiella pneumoniae* 52145 strains, used in the current study.

REFERENCES

1. Slama TG. Gram-negative antibiotic resistance: there is a price to pay. Crit Care. 2008; 12(Suppl 4):S4. [PubMed: 18495061]
2. Argyres MI. Hospital-Acquired Infections Due to Gram-Negative Bacteria. New Engl. J. Med. 2010; 363:1483–1483. [PubMed: 20931682]
3. Peters BM, Shirtliff ME, Jabra-Rizk MA. Antimicrobial Peptides: Primeval Molecules or Future Drugs? PloS Pathog. 2010; 6:e1001067. [PubMed: 21060861]
4. Wright JR. Immunoregulatory functions of surfactant proteins. Nat. Rev. Immunol. 2005; 5:58–68. [PubMed: 15630429]
5. Yang L, Johansson J, Ridsdale R, Willander H, Fitzen M, Akinbi HT, Weaver TE. Surfactant protein B propeptide contains a saposin-like protein domain with antimicrobial activity at low pH. J. Immunol. 2010; 184:975–983. [PubMed: 20007532]
6. Kuzmenko AI, Wu H, Wan S, McCormack FX. Surfactant protein A is a principal and oxidation-sensitive microbial permeabilizing factor in the alveolar lining fluid. J Biol. Chem. 2005; 280:25913–25919. [PubMed: 15890661]
7. Zhang S, Chen Y, Potvin E, Sanschagrin F, Levesque RC, McCormack FX, Lau GW. Comparative signature-tagged mutagenesis identifies Pseudomonas factors conferring resistance to the pulmonary collectin SP-A. PLoS Pathog. 2005; 1:259–268. [PubMed: 16322768]
8. Sánchez-Barbero F, Strassner J, García-Cañero R, Steinhilber W, Casals C. Role of the degree of oligomerization in the structure and function of human surfactant protein A. J. Biol. Chem. 2005; 280:7659–7670. [PubMed: 15615713]
9. Saenz A, Lopez-Sanchez A, Mojica-Lazaro J, Martinez-Caro L, Nin N, Bagatolli LA, Casals C. Fluidizing effects of C-reactive protein on lung surfactant membranes: protective role of surfactant protein A. FASEB J. 2010; 24:3662–3673. [PubMed: 20484671]
10. Sánchez-Barbero F, Rivas G, Steinhilber W, Casals C. Structural and functional differences among human surfactant proteins SP-A1, SP-A2 and co-expressed SP-A1/SP-A2: Role of supratrimeric oligomerization. Biochem. J. 2007; 406:479–489. [PubMed: 17542781]
11. Llobet E, Tomás JM, Bengoechea JA. Capsule polysaccharide is a bacterial decoy for antimicrobial peptides. 2008 Microbiology. 2008; 154:3877–3886. [PubMed: 19047754]
12. Sarrias MR, Roselló S, Sánchez-Barbero F, Sierra JM, Vila J, Yélamos J, Vives J, Casals C, Lozano F. A role for human Sp alpha as a pattern-recognition receptor. J Biol. Chem. 2005; 280:35391–35398. [PubMed: 16030018]
13. Casals C, Miguel E, Perez-Gil J. Tryptophan fluorescence study on the interaction of pulmonary surfactant protein A with phospholipid vesicles. Biochem. J. 1993; 296:585–593. [PubMed: 8280055]
14. Akinbi HT, Epaud R, Bhatt H, Weaver TE. Bacterial killing is enhanced by expression of lysozyme in the lungs of transgenic mice. J. Immunol. 2000; 165:5760–5766. [PubMed: 11067934]
15. Lin S, Na CL, Akinbi HT, Apsley KS, Whitsett JA, Weaver TE. Surfactant protein B (SP-B) −/− mice are rescued by restoration of SP-B expression in alveolar type II cells but not Clara cells. J. Biol. Chem. 1999; 274:19168–19174. [PubMed: 10383422]
16. Yan H, Hancock RE. Synergistic interactions between mammalian antimicrobial defense peptides. Antimicrobial Agents Chemother. 2001; 45:1558–1560.
17. Singh PK, Tack BF, McCray PB Jr. Welsh MJ. Synergistic and additive killing by antimicrobial factors found in human airway surface liquid. Am J Physiol Lung Cell Mol Physiol. 2000; 279:L799–805. [PubMed: 11053013]

18. Tripathi S, Tecle T, Verma A, Crouch E, White M, Hartshorn KL. The human cathelicidin LL-37 inhibits influenza A viruses through a mechanism distinct from that of surfactant protein D or defensins. J. Gen. Virol. 2013; 94:40–49. [PubMed: 23052388]
19. Ahn VE, Faull KF, Whitelegge JP, Fluharty AL, Privé GG. Crystal structure of Saposin B reveals a dimeric shell for lipid binding. Proc. Natl. Acad. Sci. 2003; 100:38–43. [PubMed: 12518053]
20. Canadas O, Garcia-Verdugo I, Keough KM, Casals C. SP-A permeabilizes lipopolysaccharide membranes by forming protein aggregates that extract lipids from the membrane. Biophys. J. 2008; 95:3287–3294. [PubMed: 18599636]
21. Mahalka AK, Kinnunen PK. Binding of amphipathic alpha-helical antimicrobial peptides to lipid membranes: lessons from temporins B and L. Biochim. Biophys. Acta. 2009; 1788:1600–1609. [PubMed: 19394305]
22. Jang H, Arce FT, Mustata M, Ramachandran S, Capone R, Nussinov R, Lal R. Antimicrobial protegrin-1 forms amyloid-like fibrils with rapid kinetics. Biophys. J. 2011; 100:1775–1783. [PubMed: 21463591]
23. Frank CG, Reguerio V, Rother M, Moranta D, Maeurer AP, Garmendia J, Meyer TF, Bengoechea JA. Klebsiella pneumoniae targets an EGF receptor-dependent pathway to subvert inflammation. Cellular Microbiol. 2013; 15:1212–1233.
24. Regueiro V, Moranta D, Frank CG, Larrarte E, Margareto J, March C, Garmendia J, Bengoechea JA. Klebsiella pneumoniae subverts the activation of inflammatory responses in a NOD1-dependent manner. Cellular Microbiol. 2011; 13:135–153.
25. Greenberger MJ, Kunkel SL, Strieter RM, Lukacs NW, Bramson J, Gauldie J, Graham FL, Hitt M, Danforth JM, Standiford TJ. IL-12 gene therapy protects mice in lethal Klebsiella pneumonia. J. Immunol. 1996; 157:3006–3012. [PubMed: 8816409]
26. Balamayooran G, Batra S, Theivanthiran B, Cai S, Pacher P, Jeyaseelan S. Intrapulmonary G-CSF rescues neutrophil recruitment to the lung and neutrophil release to blood in Gram-negative bacterial infection in MCP-1−/− mice. J. Immunol. 2012; 189:5849–5859. [PubMed: 23129755]
27. Kolaczkowska E, Kubes P. Neutrophil recruitment and function in health and inflammation. Nat. Rev. Immunol. 2013; 13:159–175. [PubMed: 23435331]
28. Niyonsaba F, Suzuki A, Ushio H, Nagaoka I, Ogawa H, Okumura K. The human antimicrobial peptide dermcidin activates normal human keratinocytes. Br. J. Dermat. 2009; 160:243–249.
29. Mansour SC, Pena OM, Hancock RE. Host defense peptides: front-line immunomodulators. Trends Immunol. 2014; 35:443–450. [PubMed: 25113635]
30. Reidy MF, Wright JR. Surfactant protein A enhances apoptotic cell uptake and TGF-beta1 release by inflammatory alveolar macrophages. Am. J. Physiol. Lung Cell Mol. Physiol. 2003; 285:L854–L861. [PubMed: 12794007]

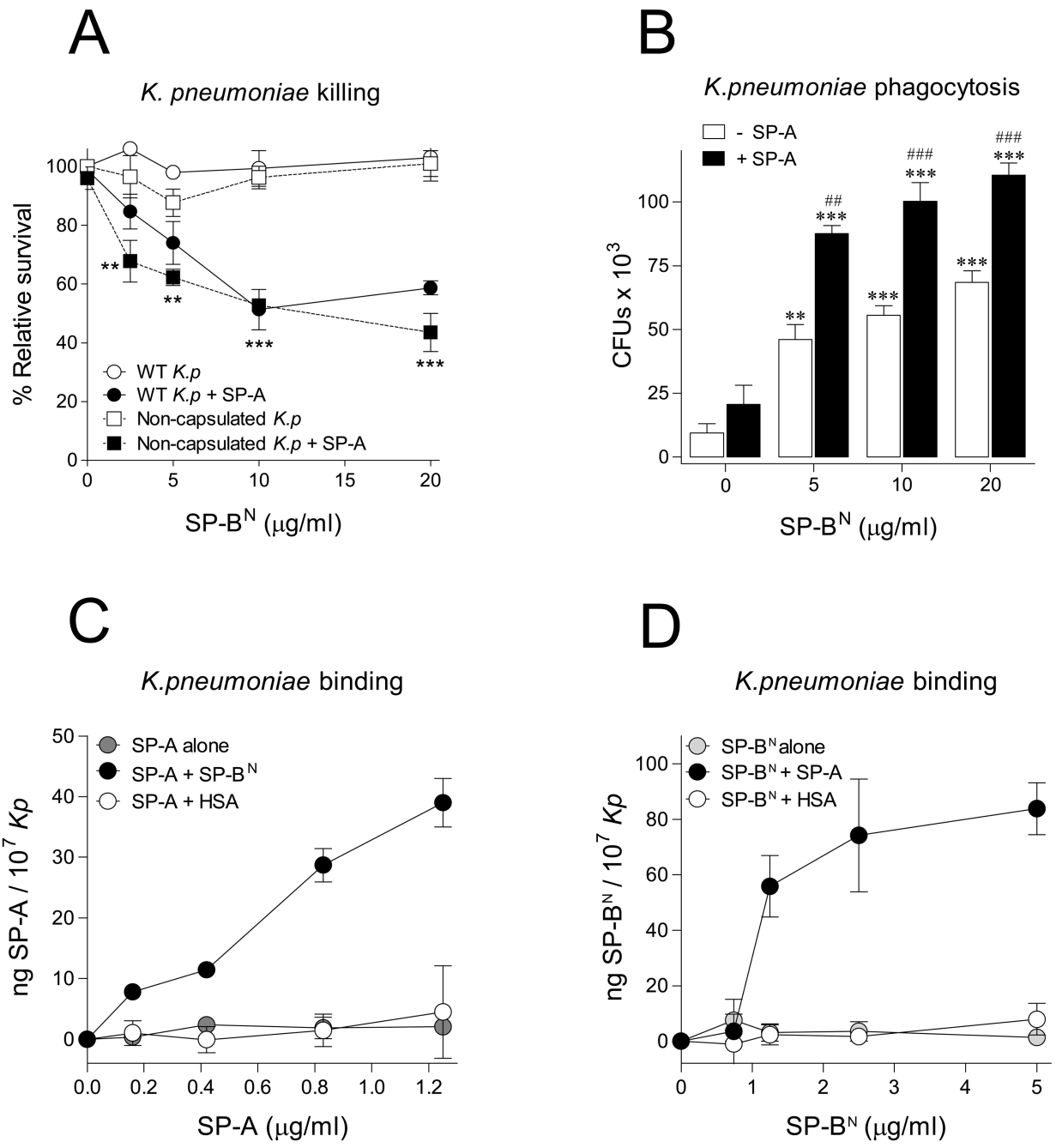

Figure 1. Synergic actions of SP-B^N and SP-A against *Klebsiella pneumoniae* at neutral pH

A) 10^5 CFUs/ml of non-capsulated or capsulated *K. pneumoniae* K2 (WT) were incubated for 1h at 37 °C with increasing concentrations of SP-B^N in the absence or presence of 100 μg/ml SP-A, in 20 mM phosphate buffer, pH 7, 150 mM NaCl. Then bacteria were plated on LB agar for CFU count after 18 h of incubation at 37 °C. Results are shown as % viable bacteria (percentage of live colony counts compared to untreated control) and are means ± SD of 4 experiments, each duplicated. A *p* value <0.0001 was obtained for overall ANOVA (Bonferroni-corrected *p* values: ***p* < 0.01, ****p* < 0.001 *vs*. the corresponding group

without SP-A). B) RAW 264.7 macrophages were pre-incubated with SP-B^N (0 to 20 μg/ml) with or without 100 μg/ml SP-A for 4 h. Cells were washed twice with PBS and infected 1 h with *K. pneumoniae* K2 (5×10^7 CFU). After infection, monolayer cells were washed 3 times with PBS, media was replaced, and 300 μg/ml gentamicin and 15 μg/ml polymyxin B were added to kill extracellular *K. pneumoniae*. Cells were lysed with 0.5% PBS-saponin and the number of viable bacteria was assessed by quantitative culture of cell lysates. Similar results were found using MH-S macrophages. Results are means ± SD of 4 experiments, each duplicated. A p value <0.0001 was obtained for overall ANOVA (Bonferroni-corrected p values: $^{**}p < 0.01$, $^{***}p < 0.001$ *vs*. the untreated infected group; ## $p < 0.01$ and ### $p < 0.001$, when comparing SP-B^N+SP-A treated *vs*. SP-B treated groups). C) Increasing concentrations of biotinylated SP-A were incubated alone (●) or in the presence of SP-B^N 10 μg/ml (●) or HSA 10 μg/ml (○) with 10^7 CFU of *K. pneumoniae K2* at room temperature for 30 minutes. Total *Klebsiella*-associated SP-A was measured by solid-phase assay and expressed as total nanograms of SP-A/10^7 bacteria. Results are means ± SD of 4 experiments, each one duplicated. D) Increasing concentrations of biotinylated SP-B^N were incubated alone (●) or in the presence of SP-A 100 μg/ml (●) or HSA 10 μg/ml (○) with 10^7 CFU of *K. pneumoniae* K2 at room temperature for 30 minutes. Total *Klebsiella*-associated SP-B^N at neutral pH was measured by solid-phase assay as reported before. Results are means ± SD of 4 experiments, each one duplicated.

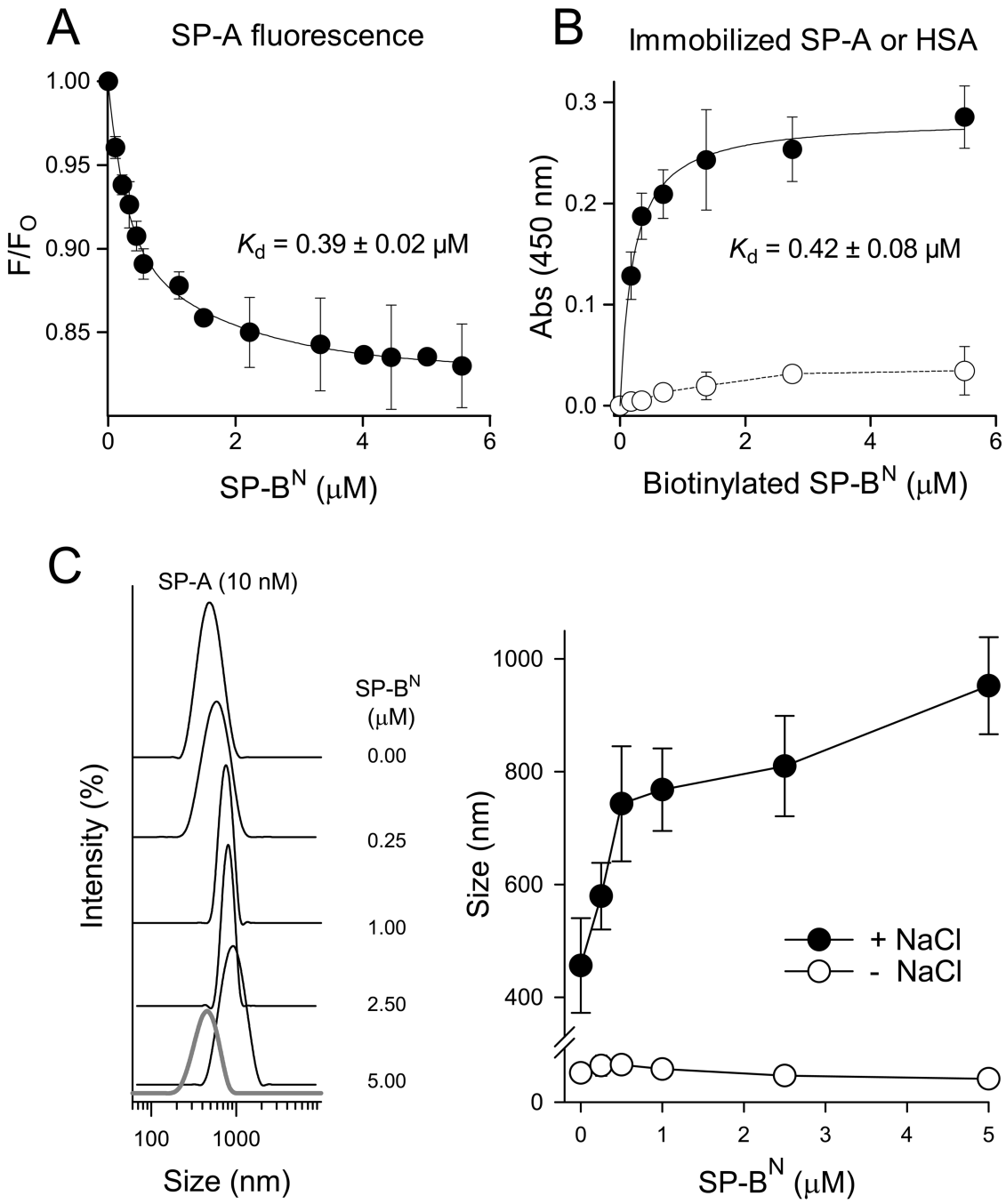

Figure 2. SP-A and SP-B^N interact in a dose-dependent manner

A) Trytophan fluorescence emission spectra of SP-A (15 nM) (10 μg/ml) were measured with or without increasing concentrations of SP-B^N (0 to 5.55 μM) (0-44 μg/ml) at 25 °C in 5 mM Tris HCl buffer (pH 7.4) containing 150 mM NaCl. SP-A samples (with and without SP-B^N) and blank samples (SP-B^N alone) were excited at 295 nm and the emission spectra recorded from 300 to 400 nm. Results are expressed as F/F$_0$, where F and F$_0$ are the corrected emission intensities at 335 nm in the presence and absence of SP-B^N. Results are means ± SD of 4 experiments. B) 25 μg of SP-A (●) or 25 μg of human serum albumin

(HSA) (○) was coated onto microtiter plate wells, and biotinylated SP-B^N (0 to 5.55 μM) was then added to the wells. The level of bound SP-B^N was determined with streptavidin-horseradish peroxidase. Results are means ± SD of 4 experiments. C) DSL analysis of the hydrodynamic diameter of SP-A/SP-B^N complexes in the presence of NaCl. (*Left*) Addition of increasing concentrations of SP-B^N (ranging from 0 to 5 μM) to a solution containing a constant concentration of SP-A (10 nM) (7μg/ml) caused an SP-B^N concentration-dependent increase of the SP-A peak. The y axis represents the relative intensity of the scattered light; the x axis denotes the hydrodynamic diameter of the particles present in the solution. SP-B^N particles alone are in gray line. One representative experiment of 4 is shown. (*Right*) The formation of SP-A/SP-B^N complexes is dependent of the presence of salts. Results are means ± SD of 4 experiments.

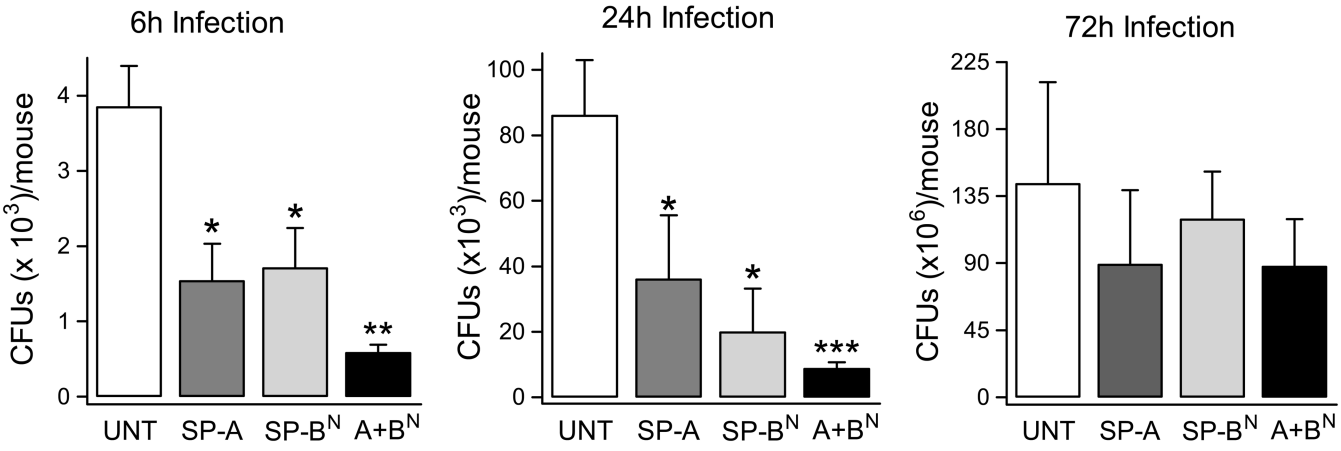

Figure 3. SP-A and SP-B^N treatment enhances bacterial clearance in mice infected with *K. pneumoniae* K2

10^4 CFUs of *K. pneumoniae* K2 were co-administered with SP-A (100 μg), SP-B^N (20 μg), or SP-A (100 μg) + SP-B^N (20 μg) in WT FVB/N mice. Lungs were harvested, weighed, and homogenized at indicated time points. The numbers of viable bacteria were assessed by colony counting and expressed as CFUs/mouse (n=6 mice each group). Results are means ± SEM. *P* values of 0.0009 (6 h infection) and 0.0002 (24 h infection) were obtained for overall ANOVA (Bonferroni-corrected *p* values: ***$p < 0.001$, **$p < 0.01$, and *$p < 0.05$ *vs*. the untreated infected group).

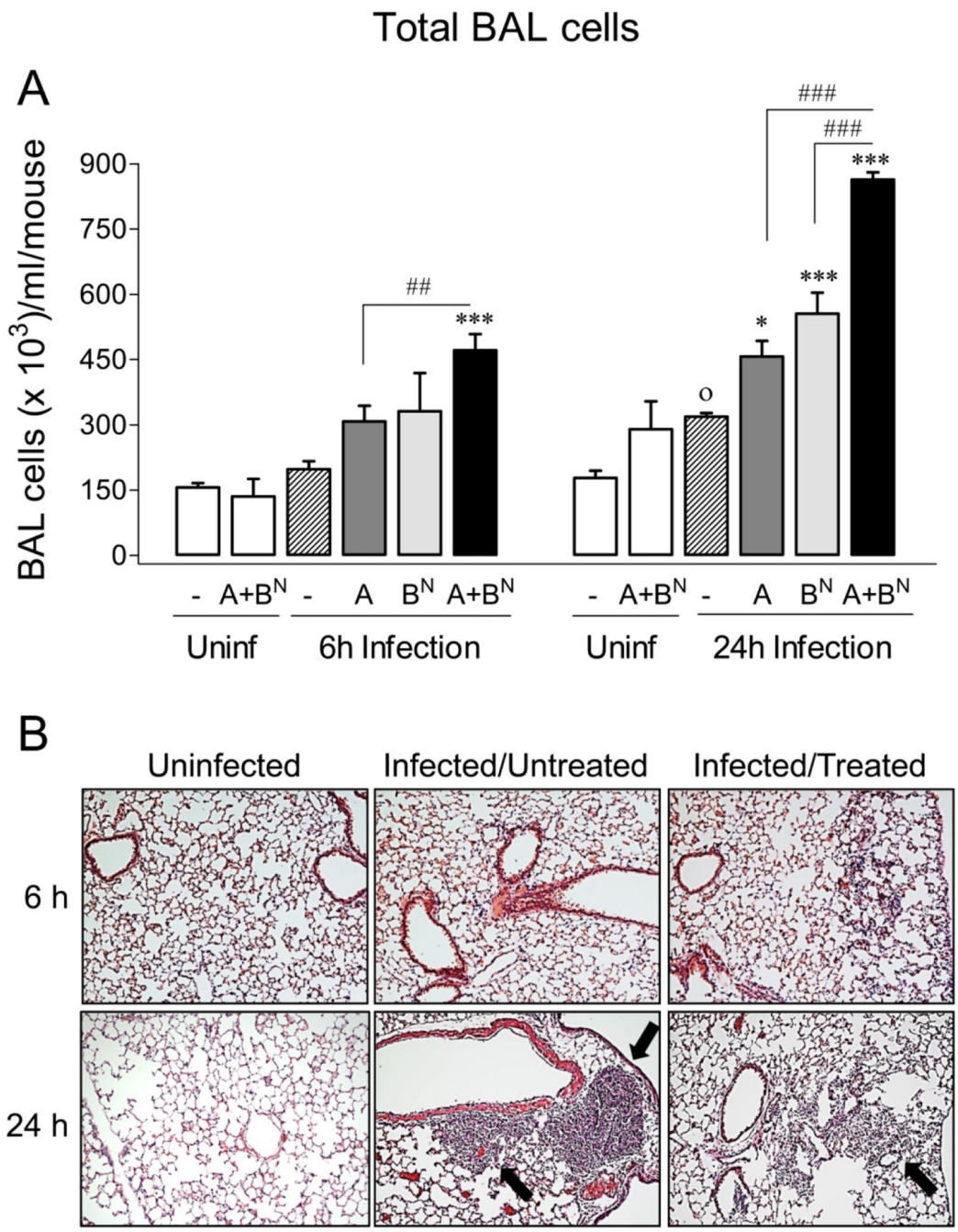

Figure 4. Effect of SP-A and SP-B^N treatment on total BAL cell count (A) and lung histopathology (B) in *K. pneumoniae* K2 infected mice

WT FVB/N mice were instilled with buffer or infected with 10^4 CFUs of *K. pneumoniae* K2 with or without SP-A (100 μg), SP-B^N (20 μg), or SP-A (100 μg) + SP-B^N (20 μg). Mice were sacrificed at 6h or 24h post-infection. (A) Total cell count in BAL were assessed (n=6 mice for each group). Results are means ± SEM. A p value <0.0001 was obtained for overall ANOVA. Bonferroni-corrected p values: *$p < 0.05$, ***$p < 0.001$ when compared with the untreated infected group; ## $p < 0.01$, ### $p < 0.001$, when comparing SP-B^N+SP-A treated

vs. SP-B or SP-A treated infected groups; $^{o}p < 0.05$ when untreated infected *vs*. uninfected groups are compared). (B) Lung sections from uninfected, infected/untreated and infected/treated (SP-A + SP-B^{N}) were stained with hematoxylin and eosin. These are representative sections of six mice in each experiment with similar results. Arrows indicate areas of lobular pneumonia. Original magnification × 10.

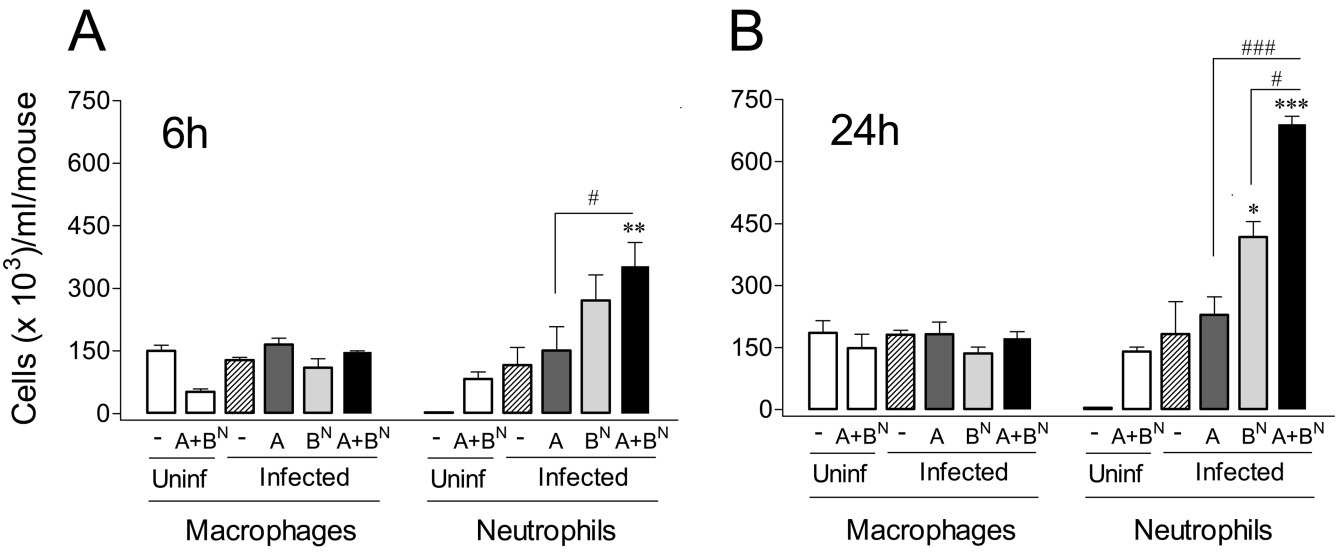

Figure 5. SP-A and SP-B^N treatment enhances early neutrophil recruitment in infected mice

WT FVB/N mice were instilled with buffer or infected with 10^4 CFUs of *K. pneumoniae* K2 with or without SP-A (100 μg), SP-B^N (20 μg), or SP-A (100 μg) + SP-B^N (20 μg). Mice were sacrificed at 6h or 24h post-infection and total alveolar macrophage and neutrophil count in BAL were assessed. Six mice were evaluated for each group at each time point. Results are means ± SEM. A p value < 0.0001 was obtained for overall ANOVA (6 h and 24 h infection). Bonferroni-corrected p values: *$p < 0.05$, ***$p < 0.001$ when compared with the untreated infected group; # $p < 0.05$, ### $p < 0.001$, when SP-B^N+SP-A treated *vs*. SP-B or SP-A treated infected groups are compared.

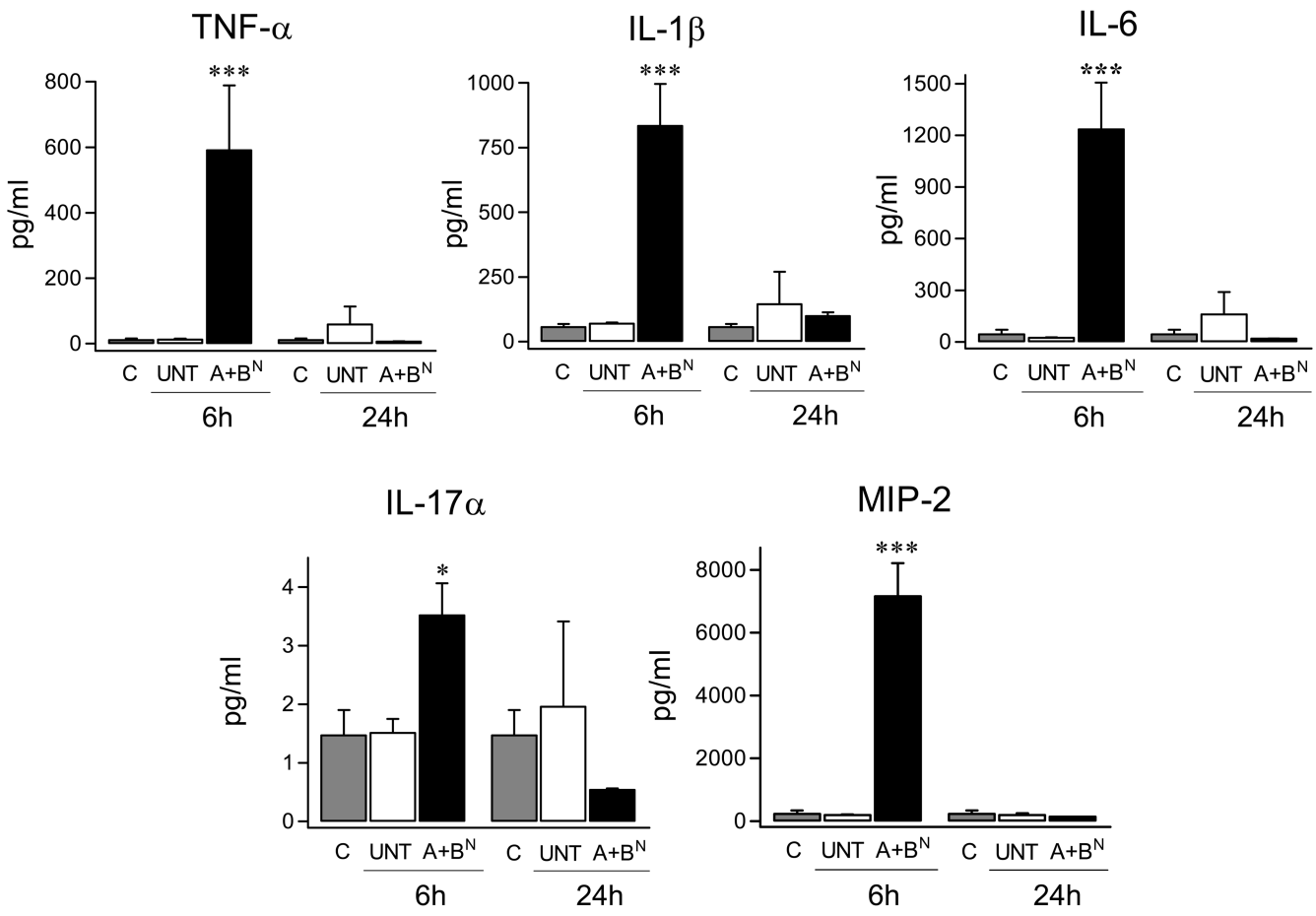

Figure 6. Early proinflammatory cytokine response in infected mice treated with SP-A/SP-B^N

WT FVB/N mice were instilled with buffer (gray bars) or 10^4 CFUs of *K. pneumoniae* K2 without (white bars) or with (black bars) 100 μg of SP-A + 20 μg of SP-B^N. Lungs were harvested at 6h and 24 hours post-infection. Concentrations of several cytokines in lung homogenates were quantified by ELISA (n = 5 mice for each group). Results are means ± SEM. A p value < 0.001 was obtained for overall ANOVA for TNF-, IL-1β, IL-6, and MIP-2 assays. For the IL-17 analysis, the p value was equal to 0.0078. Bonferroni-corrected p values: *$p < 0.05$ and ***$p < 0.001$ *vs.* all others.

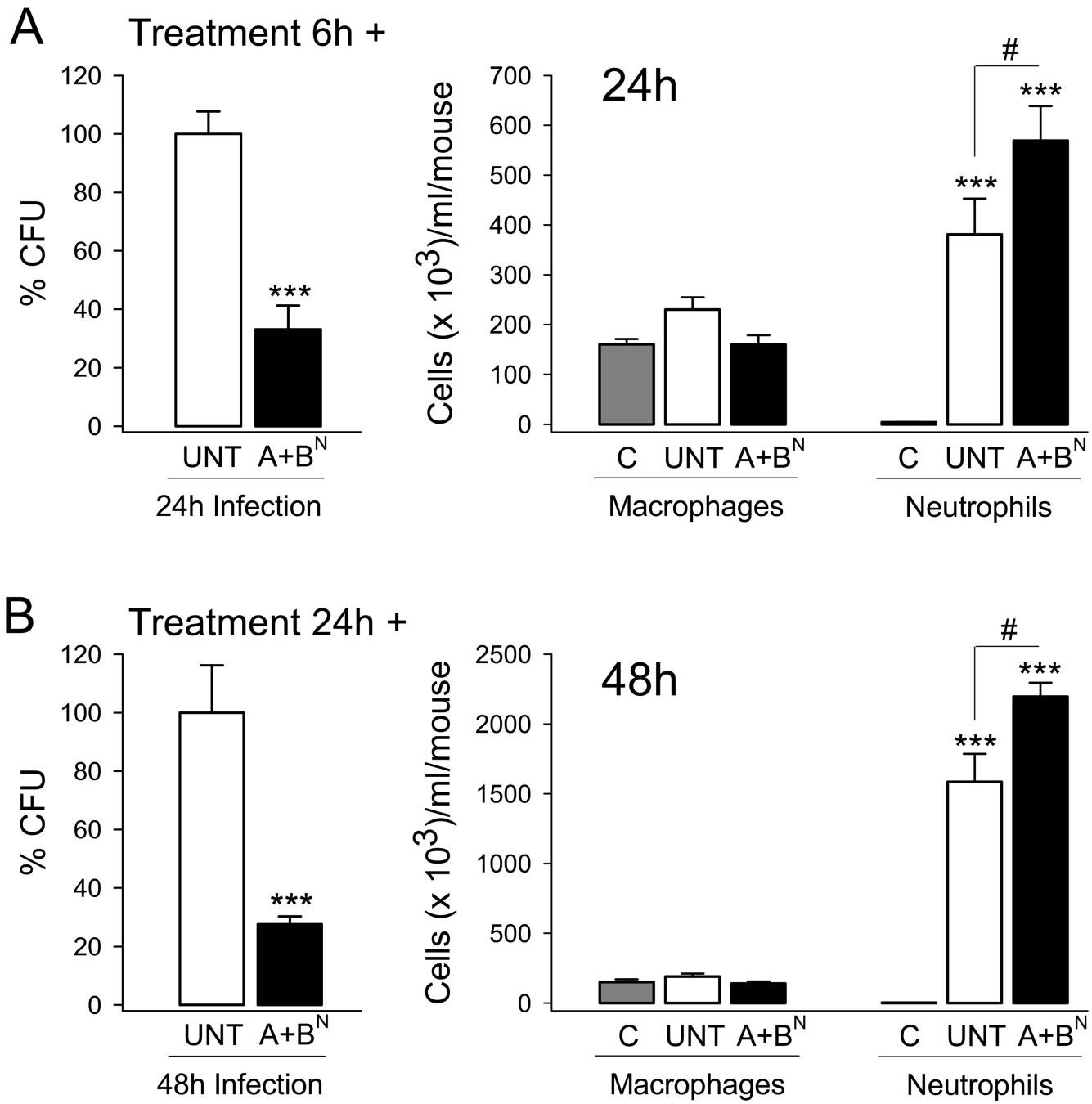

Figure 7. Therapeutic administration of SP-A/SP-B^N increases bacterial clearance and neutrophil recruitment in mice with an established K. pneumoniae K2 infection

WT FVB/N mice were instilled with buffer (control) or 10^4 CFUs of *K. pneumoniae* K2. Infected mice were treated with buffer (white bars) or SP-A (100 μg) + SP-B^N (20 μg) (black bars) 6h (A) or 24h (B) after the bacterial challenge. Mice were sacrificed at 24h (A) or 48h (B) post-infection, respectively, to assess lung bacterial burden in lungs. The numbers of viable bacteria were assessed by colony counting and expressed as CFUs/mouse. Results are means ± SEM (n=6 mice for each group). Differences in means between SP-

B^N+SP-A treated *vs*. untreated infected groups were evaluated by Student t test (***p < 0.001 *vs*. untreated group). In addition, total alveolar macrophage and neutrophil count in BAL were assessed. Results are means ± SEM. (n = 6). A p value < 0.0001 was obtained for overall ANOVA (24 h and 24 h infection). Bonferroni-corrected p values: ***p < 0.001 when compared with the uninfected group; # p < 0.05 when comparing SP-B^N+SP-A treated *vs*. untreated infected mice.